

# New terahertz dielectric spectroscopy for the study of aqueous solutions

Deepu K. George, Ali Charkhesht, and N. Q. Vinh<sup>a)</sup>

*Department of Physics, Virginia Tech, Blacksburg, Virginia 24061, USA*

(Received 6 August 2015; accepted 22 November 2015; published online 11 December 2015)

We present the development of a high precision, tunable far-infrared (terahertz) frequency-domain dielectric spectrometer for studying the dynamics of biomolecules in aqueous solutions in the gigahertz-to-terahertz frequency. As an important benchmark system, we report on the measurements of the absorption and refractive index for liquid water in the frequency range from 5 GHz to 1.12 THz (0.17–37.36  $\text{cm}^{-1}$  or 0.268–60 mm). The system provides a coherent radiation source with power up to 20 mW in the gigahertz-to-terahertz region. The dynamic range of our instrument reaches  $10^{12}$  and the system achieves a spectral resolution of less than 100 Hz. The temperature of samples can be controlled precisely with error bars of  $\pm 0.02$  °C from 0 °C to 90 °C. Given these attributes, our spectrometer provides unique capabilities for the accurate measurement of even very strongly absorbing materials such as aqueous solutions. © 2015 AIP Publishing LLC. [<http://dx.doi.org/10.1063/1.4936986>]

## I. INTRODUCTION

Terahertz frequency radiation provides unique opportunities to probe the picosecond to nanosecond time scale dynamics properties of biomaterials in liquid water.<sup>1–3</sup> The dissolved biomolecules exhibit low-frequency collective vibrational modes corresponding to conformational changes of biomolecules, such as the twisting and deformation of the DNA double-helix structure that can be probed directly by the terahertz radiation.<sup>4</sup> It has been suggested that these low-frequency modes in hydrated biomolecules efficiently direct reactions and energy transport in biological systems. Nonetheless, detailed knowledge of the structure and dynamics of biomolecules in aqueous solutions remains to be an outstanding problem in the physical and biological sciences. Furthermore, in the basic case, our understanding of the translational and rotational diffusion of water molecules and larger-scale rearrangements of their hydrogen-bonding network appears to be incomplete as significant debates exist regarding the vibrational and relaxational responses of water molecules at the femtosecond to picosecond time scales.<sup>1,3,5–7</sup> Unlike infrared and Raman spectroscopies, which are sensitive to femtosecond-scale intramolecular dynamics (i.e., bond vibrations), spectroscopy in the terahertz regime is sensitive to picosecond intermolecular solvent dynamics (i.e., molecular rotations associated with hydrogen bond breaking) as well as internal motions of solvated biomolecules. Spectroscopy in this regime thus provides a new window to study the dynamics of hydrated biomolecules, bulk solvent, and the water in the hydration shells of dissolved biomolecules. Unfortunately, the extremely strong absorbance of water, technical limitations associated with this frequency range, and often severe interference artifacts have reduced the precision of prior terahertz spectroscopy studies. These obstructions

limit our ability to characterize the largest-scale, most strongly interacting dynamic modes.

On the optical side of the electromagnetic spectrum, a number of techniques have been reported for the absorption as well as refractive spectroscopy in the terahertz region. Fourier transform spectrometer (FTS) or Michelson interferometer is a popular technique for broad frequency applications in the infrared to mid-infrared frequencies. This technique obtains information on both the refractive index and the absorption properties of the sample. The technique employs a broadband radiation source which can cover the far-infrared or the terahertz region. However, the power of a typical light source at terahertz frequencies is very weak, limiting the signal-to-noise ratio of the technique in this region. Liquid water is highly absorbing in the terahertz frequencies; thus, measurements have been done with a thin layer of water in the transmission<sup>8,9</sup> or in the reflection<sup>10,11</sup> configurations. In order to increase the signal-to-noise ratio of the method in the terahertz region, measurements have been performed using far-infrared gas lasers containing methanol or methyl iodide at low pressures with powers of several mW.<sup>12,13</sup> This method is limited to a number of discrete wavelengths depending on the gas (typically, a few laser wavelengths from 95  $\mu\text{m}$  to 1258.3  $\mu\text{m}$ ) due to discrete rotational transitions.

Recently, the absorption of liquid water using free-electron lasers,<sup>14</sup> synchrotrons,<sup>15</sup> and a germanium laser<sup>16</sup> with high radiation power at terahertz frequencies has been reported. However, the lasers provide only limited tunability over a short range of frequencies and only the absorbance (not the refractive index) of the liquid water could be extracted from the measurements. In some previous studies on protein solutions,<sup>17,18</sup> attempts have been made to extract the protein absorption coefficient by directly comparing it with that of a blank buffer. These treatments assumed that the absorption of the solution is a weighted sum of the absorption of its constituents. This assumption is not physically justified especially when the refractive index changes rapidly with

<sup>a)</sup>Electronic mail: Vinh@vt.edu

frequency as in the case of aqueous solutions in the terahertz frequencies.<sup>7,19–22</sup>

In terahertz time-domain spectroscopy,<sup>22–26</sup> typically a femtosecond laser pulse generates a fast current pulse ( $\sim 1$  ps) in a dipole antenna fabricated on low-temperature grown GaAs. This leads to the emission of electromagnetic pulse. The waveform is then Fourier transformed to obtain the power spectrum in the terahertz range from 200 GHz to several THz, depending on the material, the structure of the antenna, and the duration of the fs pulse. It is a fast method with good reproducibility and it yields information on the real and imaginary components (or the absorption and refractive index) of materials. The disadvantage is the steep power roll-off leading to a low signal-to-noise ratio for higher frequencies in the terahertz region.

On the microwave side of the spectrum, dielectric spectroscopy has been employed to provide information on the microstructure and molecular dynamics of liquid systems, especially for aqueous solutions. Barthel *et al.*<sup>27</sup> and Kaatzte<sup>28</sup> used a microwave waveguide interferometer in the transmission configuration and a coaxial-line reflection probe to obtain the dielectric relaxation spectra of water up to 89 GHz. The techniques measure simultaneously the absorption and refractive index of solution samples in a broad frequency range but are limited to the GHz frequency. In summary, the main problem in the terahertz spectroscopy is the lack of high power, high dynamics range, high resolution, and a large tunable frequency of radiation sources that limit us to study the conformational dynamics of biomolecules in the living environment.

Here, we introduce our terahertz frequency-domain spectrometer, which combines the important elements of a high dynamics range with high power, tunable frequency, and broadband emission in a table top experiment, demonstrating accurate absorption and refractive index measurements of aqueous solutions. We demonstrate that the terahertz frequency-domain spectrometer is a powerful tool for the dielectric spectroscopy in the gigahertz-to-terahertz frequency. As a first fundamental test sample, we have studied pure water. Water plays an active and complex role in sustaining life and without it, cell function would cease to exist. A deeper understanding of water will shed light on the physics and functions of biological machinery and self-assembly. However, the experimental literature describing the dynamics of water is often contradictory.<sup>18,29–32</sup> The large dynamic range of our system eliminates the severe restriction on the sample thickness that is typical to most terahertz spectrometers and therefore minimizes problems associated with multiple reflections of the incident light (standing waves and etalon effect). We have measured the absorption and refractive index of water and aqueous solutions over three orders of magnitude range from gigahertz to terahertz frequencies. The system closes the gap between the microwave region and the mid-infrared region which is well established by the FTIR technique.

## II. EXPERIMENTAL SETUP

In an effort to improve our understanding of the picosecond dynamics of water and solvated molecules, we have built a gigahertz-to-terahertz frequency-domain dielectric

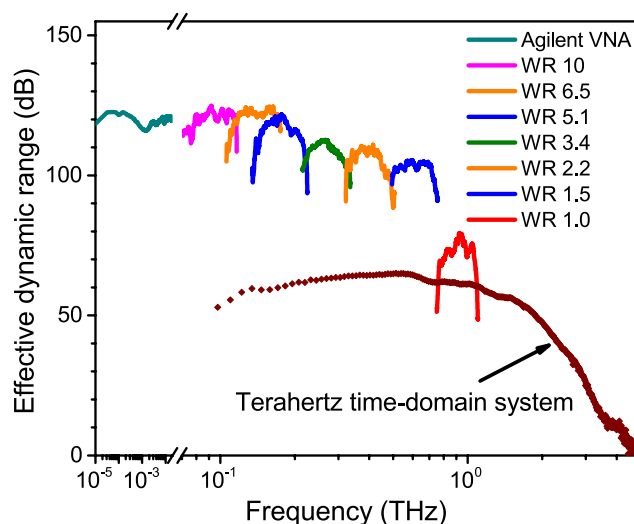


FIG. 1. Dynamic range of our gigahertz-to-terahertz frequency-domain spectrometer (Agilent vector network analyzer and frequency extenders from WR10 to WR1.0 systems) is compared with the dynamic range of a typical terahertz time-domain system. For WR10, WR5.1, WR6.5, and WR3.4 bands, we obtain the dynamic range measurements using a DUT with 30 dB loss.

spectrometer that supports the simultaneous measurements of absorbance and refractive index of solutions over the spectral range from 5 GHz to 1.12 THz ( $0.17\text{--}37.36\text{ cm}^{-1}$  or  $0.268\text{--}60\text{ mm}$ ). The signal-to-noise ratio and spectral resolution of this device are significantly improved relative to any previous state-of-the-art instruments. For example, while the dynamic range of a commercial terahertz time-domain spectrometer is just  $10^6$  and its spectral resolution is several gigahertz, the dynamic range of our instrument reaches an unprecedented value of  $10^{12}$  and the system achieves a spectral resolution of less than 100 Hz (Fig. 1). The system provides a coherent radiation source with a power up to 20 mW in the gigahertz-to-terahertz region. With the high power, we are able to measure thick layers up to 2 mm of liquid water. The temperature of the liquid sample can be controlled with high accuracy of ( $\pm 0.02$ ) °C. Given these attributes, our spectrometer provides unique capabilities for the accurate measurement of even very strongly absorbing materials such as aqueous solutions.<sup>7,19</sup>

Our spectrometer consists of a commercial Vector Network Analyzer (VNA) from Agilent, the N5225A PNA, which covers the frequency range from 10 MHz to 50 GHz, and frequency multipliers and the matched harmonic detectors for terahertz radiation, which are developed by Virginia Diodes, Inc. (Charlottesville, VA). Detailed information on the vector network analyzer frequency extension modules and the mixer process can be obtained elsewhere.<sup>33,34</sup> The principle of the frequency extender terahertz modules is shown in Fig. 2. Instead of using optical sources and mixing down the frequency to access the terahertz range, the terahertz radiation in this case is generated by up-converting frequencies from microwave sources. The frequency multipliers are fabricated using Schottky diode based components.<sup>34</sup> The transmitter module allows us to up-convert an arbitrary signal from a vector network analyzer in the frequency range between 10 MHz and 50 GHz to the terahertz frequency region and

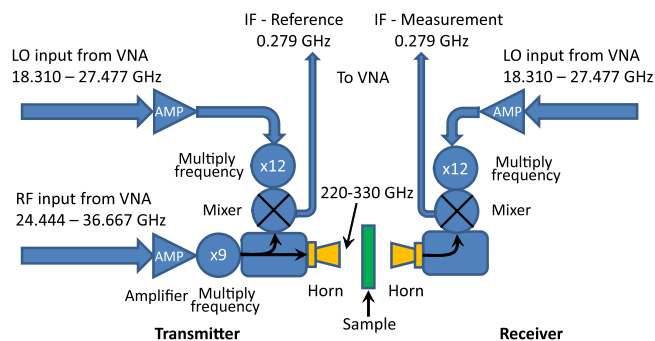


FIG. 2. Block diagram of the WR3.4 (220–300 GHz) transmitter and receiver frequency extender modules. The microwave source from Agilent vector network analyzer is extended via custom Virginia Diode frequency extenders to cover up to 1.12 THz.

transmits it with a rectangular-to-circular horn antenna into free-space. Specifically, in Fig. 2, the RF (radio frequency) input from a VNA with frequency range from 24.444 to 36.667 GHz enters the WR3.4 frequency extension modules for up conversion frequency by nine times to 220–330 GHz. At the receiver module, a second horn antenna serves to receive the signal after a sample and feeds it into the mixer for down conversion. The transmitted as well as received signals mix with a Local Oscillator (LO) from the VNA in a subharmonic mixer. The resulting Intermediate Frequency (IF) signals from the transmitter and receiver detected by the VNA determine the intensity and phase of the reference and measurement signals. In this case, the IF signals are the difference between up-converted signals of RF and LO signals at 0.279 GHz. Our terahertz sources from Virginia Diodes for the WR3.4 frequency extension module produce several milliwatts of power at 300 GHz. The dynamic range for this frequency band of 110 dB can be achieved with a device under test (DUT) of 30 dB loss (Fig. 1).

The spectrometer provides a large range of frequencies from gigahertz to terahertz with the output power up to 20 mW. The frequency extenders consist of commercial frequency extenders and matched harmonic receivers from Virginia Diodes, Inc., including WR10, WR6.5, WR5.1, WR3.4, WR2.2, WR1.5, and WR1.0 to cover the frequency range from 60 GHz to 1.12 THz. The dynamic range of the instrument reaches  $10^{12}$  with a spectral resolution of less than 100 Hz (Fig. 1). The lower frequency bands including WR10, WR5.1, WR6.5, and WR3.4 have high output power up to 20 mW; thus, we obtain the dynamic measurements for these bands using a DUT with 30 dB loss. For convenience to change frequency bands, the output radiation from WR6.5, WR5.1, WR3.4, WR2.2, WR1.5, and WR1.0 frequency extenders are transformed into the rectangular WR10 waveguide configuration with waveguide taper transitions. From the rectangular WR10 waveguide, we use a transition waveguide to transform the radiation into the circular WR10 waveguide with minimum loss and reflections. The output of the circular WR10 horn enters our sample cell (Fig. 3). The internal diameter of the circular horn is 2.85 mm and the wall thickness at the end of the horn is 2.00 mm. Thus, we can easily obtain the dielectric response from 60 GHz to 1.12 THz for liquid samples. For lower frequencies from

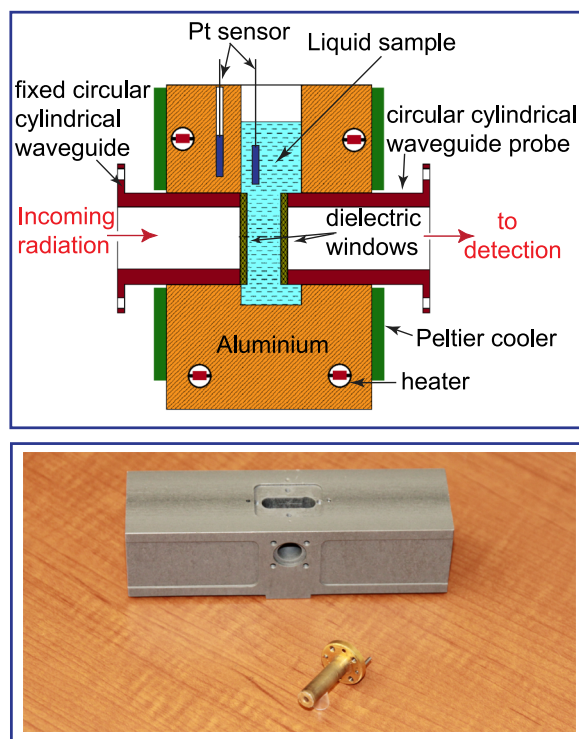


FIG. 3. A variable path-length sample cell measures how absorbance and refractive index change with changing path-length of the sample cell (top). The sample cell with the WR10 circular horn allows us to measure the dielectric response of liquid materials from 60 GHz to 1.12 THz (bottom).

5 GHz to 50 GHz, we employ directly the radiation from the VNA system into the sample cell designed for WR137 and WR28 waveguide configurations.

We have employed a variable path-length cell setup<sup>22,35</sup> consisting of two parallel windows inside an aluminum cell, one immobile and the other mounted on an ultra-precise linear translation stage (relative accuracy of 50 nm) (Fig. 3, top). Our translation stage from Newport (XMS160 ultra-precision linear Motor Stages) can perform 1 nm minimum incremental motion with a travel range of 160 mm. The linear translation stage has a direct-drive system for ultra-precision and a high accuracy linear glass scale encoder with 80 nm repeatability. We use thin polyethylene sheets of 80  $\mu\text{m}$  thickness for the two parallel windows to cover the circular side of the horn antenna with the internal diameter of 2.85 mm. The large thickness of the wall at the end of the circular waveguide allows us to glue the windows strongly so that they retain their shape during measurements (Fig. 3, bottom). The thin parallel windows avoid the multi-reflection effect to the radiation source as well as the detection part. The metal cell minimizes the leakage of stray radiation. The thickness of liquid samples or the distance between the two windows, which is the sample path-length, is adjusted using the ultra-precise linear stage. At each frequency, we examine an average of 100 different path-lengths (Fig. 4), with increments ranging from 0.1 to 20  $\mu\text{m}$ , depending on the absorption strength of the sample.

The choice of the thickness of liquid water samples depends on the dynamics of frequency bands. The thickness varies from 0.5 mm for WR1.0 to 2.0 mm for the WR10

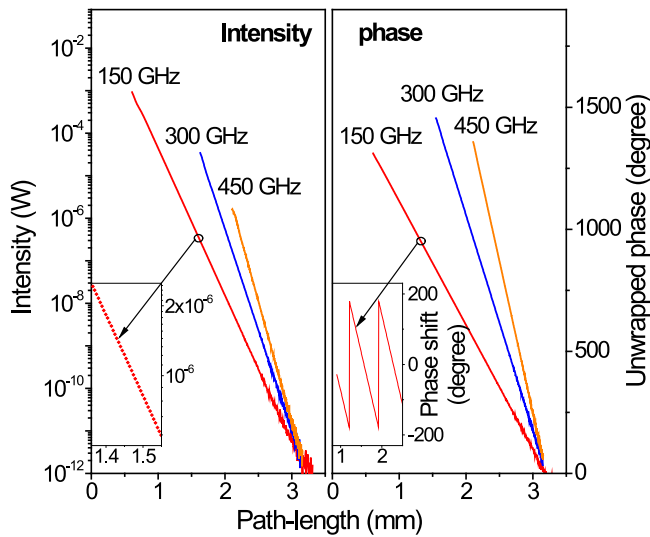


FIG. 4. The variable path-length sample cell measures the intensity (left) and the phase (right) of transmitted terahertz radiation as functions of path-length. The slopes of these lines define the absorbance coefficient and refractive index of water, respectively, without the need for knowledge of the (difficult to obtain) absolute path-length or absolute absorbance of our samples. The insets in the figure demonstrate the quality of the measurements. The data in the right inset illustrate the phase shift as a function of sample length.

band. Since the system is frequency-domain, we can use the frequency step size as small as the linewidth of the radiation (sub 100 Hz). Depending on the spectral linewidth of the material, we will choose the frequency step size. Water in the gigahertz to terahertz frequencies shows a broad band of absorption and refractive index. Typically, we use a frequency step size of 1 GHz for water measurements.

The fast performance and signal acquisition of the system of 35  $\mu$ s per frequency allow us to perform time dependent measurements. We employ the high speed Ethernet connection for data acquisition to transfer data from the VNA to computer. The time to obtain both absorption and refractive index measurements for one frequency extender system varies from 20 s to 5 min depending on the number of frequency points. For example, the time to scan from 5 GHz to 1.12 THz with an average of five times and a frequency step size of 1 GHz for water measurements (Fig. 5), we need about 3 h including measurement time and 5 min each time to change frequency extenders.

The temperature of the sample cell can be controlled precisely from 0 °C to 90 °C. The sample cell is embedded in a large metal body part of 152  $\times$  38  $\times$  18 mm (Fig. 3). The Peltier cooler plates from Custom Thermolectric (12711-5L31-03CK) and high power resistors are mounted on the body of the sample cell, allowing precise control of the temperature of the sample. The absorbance and refractive index of water are extremely sensitive to temperature, and thus all experiments are carried out with a measured accuracy of  $\pm 0.02$  °C. To mitigate problems associated with multiple reflections of the incident light (standing waves and etalon effect), the thickness of our shortest path-length was selected to be long enough to ensure strong attenuation of the incident radiation (transmission  $< 10^{-2}$ ).

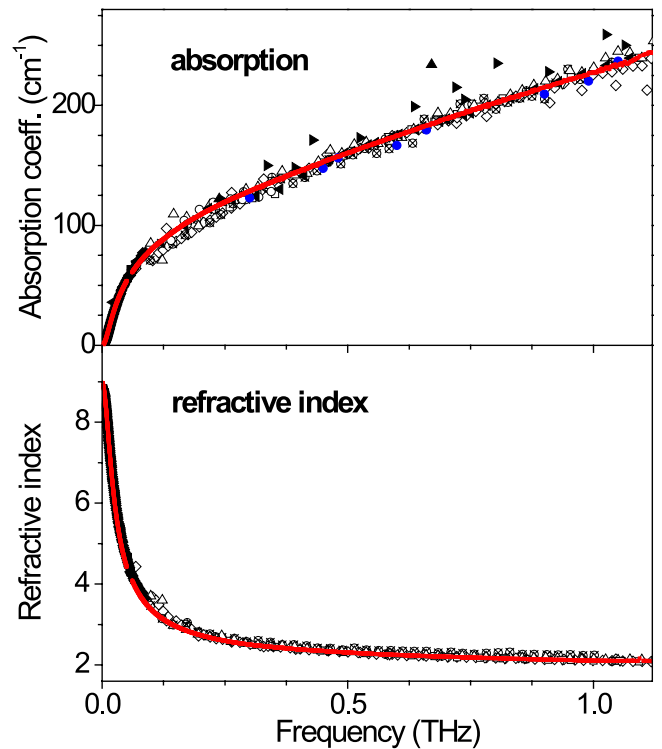


FIG. 5. The red, continuous lines in these two plots are spectra of water collected with our instrument. The error bars of absorption and refractive index measurements are within the thickness of the lines. Superimposed on these are data collected from the literature including measurements using FTIR interferometer ( $\nabla$ <sup>8</sup> and  $\blacktriangleleft$ <sup>9</sup>), reflection dispersive Fourier transform spectroscopy ( $\oplus$ <sup>10</sup> and  $\circ$ <sup>11</sup>), far-infrared lasers ( $\blacktriangle$ <sup>12</sup> and  $\blacktriangleright$ <sup>13</sup>), free-electron laser ( $\bullet$ ),<sup>14</sup> terahertz time-domain transmission ( $\diamond$ <sup>22,23</sup> and  $\square$ <sup>24</sup>) and reflection ( $\otimes$ <sup>25</sup> and  $\Delta$ <sup>26</sup>) spectroscopies, and dielectric relaxation spectroscopy ( $\blacklozenge$ <sup>27</sup> and  $\blacksquare$ <sup>28</sup>).

### III. DATA EVALUATION

#### A. Absorption and refractive index measurements

Using the above-described spectrometer and sample cell, we have measured the change of intensity and phase in aqueous samples as functions of path-length (Fig. 4). The absorption process of the terahertz radiation passing through a sample is described by Beer's law,

$$I(l, \nu) = I_0(\nu) \cdot e^{-\alpha(\nu) \cdot l}, \quad (1)$$

where  $\nu$ ,  $I_0$ ,  $I$ ,  $\alpha(\nu)$ , and  $l$  are the frequency, the incident intensity, the intensity at the detection of the radiation, the absorption coefficient as a function of radiation frequency, and the thickness of the sample, respectively. When the radiation passes through a material, it will always be attenuated. This can be conveniently taken into account by defining a complex refractive index,

$$n^*(\nu) = n(\nu) - i\kappa(\nu), \quad (2)$$

with the real part,  $n(\nu)$ , which is the refractive index and indicates the phase velocity, while the imaginary part,  $\kappa(\nu)$ , is called the extinction coefficient and indicates the amount of attenuation when the radiation propagates through the material. The extinction coefficient is related to the absorption coefficient,  $\alpha(\nu)$ , by

$$\alpha(\nu) = \frac{4\pi \cdot \nu \cdot \kappa(\nu)}{c}, \quad (3)$$

with  $c$  as the speed of light. We have measured the intensity and phase shift of water and aqueous solutions over three orders of magnitude range 5.0 GHz–1.12 THz as functions of path-length,  $l$ , at 20.00 ( $\pm 0.02$ ) °C. The absorption coefficient is determined by the slope of a linear fit of  $\ln I(l, \nu)$  to the path-length,  $l$ , without the need for precise knowledge of the sample's absolute absorbance or absolute path-length,

$$\ln I(l, \nu) = \ln I_0(\nu) - \alpha(\nu) \cdot l. \quad (4)$$

In parallel, we also fit the observed phase shift  $\theta(l, \nu)$  as a linear function of path-length to define the refractive index,  $n(\nu)$ , of the sample,

$$\theta(l, \nu) = \theta_0(\nu) + \frac{2\pi \cdot \nu \cdot n(\nu)}{c} \cdot l, \quad (5)$$

where the  $\theta_0(\nu)$  is the phase of the reference signal. Note that Eq. (5) does not have a form of  $(n(\nu) - 1)$  as in many variable path-length measurements since our detector is attached to the moving window of the sample cell. When the optical path-length of the sample is changed, the detector moves with a distance that is equivalent to the change of the geometrical length of the light traveling in the sample. Both properties of liquid water (absorption coefficient and refractive index) are strong functions of frequency, monotonically increasing and decreasing, respectively, with rising frequency over this entire spectral range (Fig. 5).

This method supports the precise determination of absorption coefficients and refractive indexes without the need for precise (and difficult to obtain) measurements of the absolute path-length and the intrinsic optical properties of the sample cell. All experiments were repeated approximately five times to estimate confidence limits. We fit the intensity data to the Beer's law, Eq. (1), to obtain values for the absorption coefficients of a sample as a function of frequency,  $\alpha$  (Fig. 4, left) with a high degree of accuracy. In parallel, fitting the observed phase shift as a linear function of path-length, Eq. (5), provides the refractive index of the sample,  $n$  (Fig. 1, right). The standard errors of the mean of replicate measurements are typically smaller than 0.2%. Using our sensitive setup, we measured precisely the absorption coefficient and refractive index of the strong absorption material, water (Fig. 5), and aqueous solutions at the terahertz frequencies. The red, continuous lines on these two plots in Fig. 5 are spectra of water collected with our instrument at 20 °C. The error bars of our absorption and refractive index measurements are within the thickness of the lines. Superimposed on these are data collected from the literature,<sup>10,11,14,22,25,36,37</sup> illustrating the vastly improved signal-to-noise ratio and spectral resolution of our instrument.

## B. Complex dielectric response of solutions

The spectroscopies cover a broadband spectral range from gigahertz to terahertz frequencies that allow us to observe both the relaxational (rotational) and translational processes of water molecules and biomolecules. Thus, the dielectric response will provide an entire picture of the

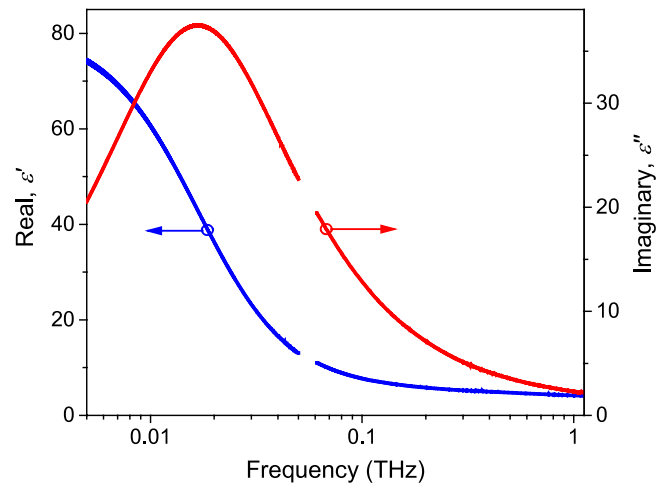


FIG. 6. The dielectric response from water at 20 °C is converted from the absorption coefficient and refractive index measurements. The error bars for the calculated dielectric response are within the thickness of the lines.

dynamics of biomolecules in the living environment. The frequency-dependent complex dielectric response,  $\epsilon^*(\nu) = \epsilon'(\nu) - i\epsilon''(\nu)$ , is related to the complex refractive index,  $n^*(\nu) = n(\nu) - i\kappa(\nu)$ , through the relations<sup>38</sup>

$$\begin{aligned} \epsilon'(\nu) &= n^2(\nu) - \kappa^2(\nu) = n^2(\nu) - (c\alpha(\nu)/(4\pi\nu))^2, \\ \epsilon''(\nu) &= 2n(\nu) \cdot \kappa(\nu) = 2n(\nu)c\alpha(\nu)/(4\pi\nu). \end{aligned} \quad (6)$$

From this, we can determine the complex dielectric function,  $\epsilon^*(\nu)$ , of the water and aqueous solutions, which in turn provides a complete description of the interaction of the solution with the incoming electromagnetic wave. Figure 6 shows the dielectric response from water at 20 °C. Conversely, given the complex dielectric response,  $\epsilon'(\nu)$  and  $\epsilon''(\nu)$ , we can determine the absorption,  $\alpha(\nu)$ , and the refractive index  $n(\nu)$ ,

$$\begin{aligned} n(\nu) &= \left( \frac{\sqrt{\epsilon'(\nu)^2 + \epsilon''(\nu)^2} + \epsilon'(\nu)}{2} \right)^{1/2}, \\ \alpha(\nu) &= \frac{4\pi\nu}{c} \left( \frac{\sqrt{\epsilon'(\nu)^2 + \epsilon''(\nu)^2} - \epsilon'(\nu)}{2} \right)^{1/2}. \end{aligned} \quad (7)$$

## IV. DISCUSSION

We have demonstrated that we are now able to determine the absorption as well as the refractive index of aqueous solutions with the dielectric terahertz spectroscopy. The system reduces the influence of interference and other systematic effects to minimum and provides reliable absolute experimental data for water and aqueous solutions. The absorption coefficient as well as the refractive index of water strongly depends on temperature. We have employed the Peltier system to control the temperature with a high accuracy of 0.02 °C. It is a fast technique that allows us to observe the conformation changes of biomolecules in solutions as a function of time.

Figure 5 shows the result of our measurement of liquid water measured at 20 °C. The absorption coefficient and

refractive index are strong functions of frequency, monotonically increasing and decreasing, respectively, with rising frequency over this entire spectral range. The red, continuous lines collected with our instrument for spectra of water are in good agreement with previously reported spectra (Fig. 5). Zelsmann<sup>8</sup> and Zoidis *et al.*<sup>9</sup> recorded the spectra of water with a FTIR interferometer in the range from 8 to 450 cm<sup>-1</sup> (239 GHz to 13.5 THz) using the transmission configuration. Afsar and Hasted<sup>10</sup> and Hasted *et al.*<sup>11</sup> employed a reflection dispersive Fourier transform spectroscopy to measure the absorption and refractive index of liquid water in the spectral range between 4 and 450 cm<sup>-1</sup> (120 GHz to 13.5 THz). Using far-infrared gas lasers with powers of several mW, Vij<sup>12</sup> and Simpson *et al.*<sup>13</sup> reported the absorption coefficients of liquid water in a few frequencies in the terahertz region. Xu *et al.*<sup>14</sup> measured the absorption coefficient of liquid water between 0.3 and 3.75 THz with free-electron lasers. Schmuttenmaer *et al.*<sup>22,23</sup> and Yada *et al.*<sup>24</sup> reported the absorption coefficient and refractive index with a terahertz time-domain system in the transmission configuration in the range from 2.0 to 60 cm<sup>-1</sup> (60 GHz to 1.8 THz) using a variable path-length sample cell. The absorption coefficient was determined by the slope of a linear regression fit of the detected intensity versus the path-length at room temperature. Thrane *et al.*<sup>25,26</sup> collected the terahertz spectrum of liquid water at 292 K using a terahertz time-domain system in the reflection configuration in the range from 3.0 to 33 cm<sup>-1</sup> (90 GHz to 1.0 THz). Barthel *et al.*<sup>27,29</sup> and Kaatze<sup>28</sup> used the microwave waveguide interferometer in the transmission configuration and coaxial-line reflection probe, reflectively, to obtain the dielectric relaxation spectra of water up to 89 GHz. Superimposed on these are data collected from the literature,<sup>10,11,13,14,22,25,36,37</sup> illustrating the significantly improved signal-to-noise ratio and spectral resolution of our terahertz spectrometer.

In summary, we have demonstrated a new method to obtain terahertz spectra of high absorption polar liquid with a high precision, high dynamics range, high resolution, and a large frequency range from gigahertz-to-terahertz region. The terahertz frequency-domain dielectric spectroscopy applied to liquid water showed good agreement with previous measurements. Using this setup, we have been able to determine the absorption coefficient and the refractive index of water as well as the aqueous biological solutions in the range between 5 GHz and 1.12 THz with high precision.

## ACKNOWLEDGMENTS

This work was supported by the Institute of Critical Technology and Applied Sciences (ICTAS) at Virginia Tech.

- <sup>1</sup>M. Chaplin, *Nat. Rev. Mol. Cell. Biol.* **7**, 861 (2006).
- <sup>2</sup>P. Ball, *ChemPhysChem* **9**, 2677 (2008).
- <sup>3</sup>D. P. Zhong, S. K. Pal, and A. H. Zewail, *Chem. Phys. Lett.* **503**, 1 (2011).
- <sup>4</sup>A. G. Markelz, A. Roitberg, and E. J. Heilweil, *Chem. Phys. Lett.* **320**, 42 (2000).
- <sup>5</sup>M. Koeberg, C. C. Wu, D. Kim, and M. Bonn, *Chem. Phys. Lett.* **439**, 60 (2007).
- <sup>6</sup>T. Wytttenbach and M. T. Bowers, *Chem. Phys. Lett.* **480**, 1 (2009).
- <sup>7</sup>N. Q. Vinh, S. J. Allen, and K. W. Plaxco, *J. Am. Chem. Soc.* **133**, 8942 (2011).
- <sup>8</sup>H. R. Zelsmann, *J. Mol. Struct.* **350**, 95 (1995).
- <sup>9</sup>E. Zoidis, J. Yarwood, and M. Besnard, *J. Phys. Chem. A* **103**, 220 (1999).
- <sup>10</sup>M. N. Afsar and J. B. Hasted, *J. Opt. Soc. Am.* **67**, 902 (1977).
- <sup>11</sup>J. B. Hasted, S. K. Husain, F. A. M. Frescura, and J. R. Birch, *Chem. Phys. Lett.* **118**, 622 (1985).
- <sup>12</sup>J. K. Vij, *Int. J. Infrared Millimeter Waves* **10**, 847 (1989).
- <sup>13</sup>O. A. Simpson, B. L. Bean, and S. Perkowitz, *J. Opt. Soc. Am.* **69**, 1723 (1979).
- <sup>14</sup>J. Xu, K. W. Plaxco, and S. J. Allen, *J. Chem. Phys.* **124**, 036101 (2006).
- <sup>15</sup>E. Giovenale, M. D'ariento, A. Doria, G. P. Gallerano, A. Lai, G. Messina, and D. Piccinelli, *J. Biol. Phys.* **29**, 159 (2003).
- <sup>16</sup>A. Bergner, U. Heugen, E. Brundermann, G. Schwaab, M. Havenith, D. R. Chamberlin, and E. E. Haller, *Rev. Sci. Instrum.* **76**, 063110 (2005).
- <sup>17</sup>S. Ebbinghaus, S. J. Kim, M. Heyden, X. Yu, U. Heugen, M. Gruebele, D. M. Leitner, and M. Havenith, *Proc. Natl. Acad. Sci. U. S. A.* **104**, 20749 (2007).
- <sup>18</sup>S. Funkner, G. Niehues, D. A. Schmidt, M. Heyden, G. Schwaab, K. M. Callahan, D. J. Tobias, and M. Havenith, *J. Am. Chem. Soc.* **134**, 1030 (2012).
- <sup>19</sup>N. Q. Vinh, M. S. Sherwin, S. J. Allen, D. K. George, A. J. Rahmani, and K. W. Plaxco, *J. Chem. Phys.* **142**, 164502 (2015).
- <sup>20</sup>T. C. Choy, *Effective Medium Theory: Principle and Applications* (Clarendon Press, Oxford, 1999).
- <sup>21</sup>D. V. Matyushov, *J. Phys. Condens. Matter.* **24**, 325105 (2012).
- <sup>22</sup>J. T. Kindt and C. A. Schmuttenmaer, *J. Phys. Chem.* **100**, 10373 (1996).
- <sup>23</sup>D. S. Venables and C. A. Schmuttenmaer, *J. Chem. Phys.* **108**, 4935 (1998).
- <sup>24</sup>H. Yada, M. Nagai, and K. Tanaka, *Chem. Phys. Lett.* **464**, 166 (2008).
- <sup>25</sup>L. Thrane, R. H. Jacobsen, P. U. Jepsen, and S. R. Keiding, *Chem. Phys. Lett.* **240**, 330 (1995).
- <sup>26</sup>C. Ronne, L. Thrane, P. O. Astrand, A. Wallqvist, K. V. Mikkelsen, and S. R. Keiding, *J. Chem. Phys.* **107**, 5319 (1997).
- <sup>27</sup>J. Barthel, K. Bachhuber, R. Buchner, and H. Hetzenauer, *Chem. Phys. Lett.* **165**, 369 (1990).
- <sup>28</sup>U. Kaatze, *J. Chem. Eng. Data* **34**, 371 (1989).
- <sup>29</sup>T. Fukasawa, T. Sato, J. Watanabe, Y. Hama, W. Kunz, and R. Buchner, *Phys. Rev. Lett.* **95**, 197802 (2005).
- <sup>30</sup>A. Y. Zasetsky, *Phys. Rev. Lett.* **107**, 117601 (2011).
- <sup>31</sup>K. J. Tielrooij, N. Garcia-Araez, M. Bonn, and H. J. Bakker, *Science* **328**, 1006 (2010).
- <sup>32</sup>W. J. Ellison, *J. Phys. Chem. Ref. Data* **36**, 1 (2007).
- <sup>33</sup>C. Jastrow, K. Munter, R. Piesiewicz, T. Kurmer, M. Koch, and T. Kleine-Ostmann, *Electron. Lett.* **44**, 213 (2008).
- <sup>34</sup>T. W. Crowe, W. L. Bishop, D. W. Porterfield, J. L. Hesler, and R. M. Weikle, *IEEE J. Solid-State Circuits* **40**, 2104 (2005).
- <sup>35</sup>J. Xu, K. W. Plaxco, and S. J. Allen, *Protein Sci.* **15**, 1175 (2006).
- <sup>36</sup>J. K. Vij, D. R. J. Simpson, and O. E. Panarina, *J. Mol. Liq.* **112**, 125 (2004).
- <sup>37</sup>G. J. Evans, M. W. Evans, P. Minguzzi, G. Salvetti, C. J. Reid, and J. K. Vij, *J. Mol. Liq.* **34**, 285 (1987).
- <sup>38</sup>J. R. Birch and J. Yarwood, *In Spectroscopy and Relaxation of Molecular Liquids* (Elsevier, Amsterdam, 1991).